

Charge-density-wave phase reconstruction in the photoinduced dynamic phase transition in $K_{0.3}MoO_3$

N. Ogawa*

Department of Applied Physics, The University of Tokyo, Tokyo 113-8656, Japan

Y. Murakami

Department of Physics, Tohoku University, Sendai 980-8577, Japan

K. Miyano

Research Center for Advanced Science and Technology, The University of Tokyo, Tokyo 153-8904, Japan

(Received 22 November 2001; published 27 March 2002)

Charge-density-wave (CDW) strain in a quasi-one-dimensional conductor $K_{0.3}MoO_3$ is studied with high-resolution x-ray diffraction. It is found that photoexcitation promotes the relaxation of the CDW strain imposed by the external electric field, which can drastically affect the dynamic phase transition of the CDW motion from a sliding state to a creep state. The deformation of the CDW structure in the creeping phase is also found.

DOI: 10.1103/PhysRevB.65.155107

PACS number(s): 71.45.Lr, 74.60.Ge, 78.70.Ck, 78.20.-e

I. INTRODUCTION

Charge-density-wave (CDW)¹ and vortex lattices in a type-II superconductor² are model systems to study the dynamic response of the elastic periodic medium under the influence of randomly distributed pinning sites. The response is governed by the interplay between deformation energy, pinning potential, and external field. In the case of a CDW, the overall evolution of the dynamic phase response can be classified into three phases:³ (1) a deformed solid at rest (pinned), (2) a plastic creep, and (3) a sliding solid. Several phase diagrams in the external force and temperature plane have been proposed.⁴ In the pinned and creep phases, the long-range order of the periodic structure is destroyed through the accumulation of internal deformation by the external field. However, it is predicted that the long-range order of the system will recover in the sliding phase because of the weakening of the effective pinning potential. Up to now, such a reordering has been found only in the vortex lattice systems.⁵ The discrepancy between theory and experiment in the CDW system remains a current problem.

We formerly reported that photoexcitation can drastically affect the creep-to-slide dynamic phase transition of the CDW in a quasi-one-dimensional conductor $K_{0.3}MoO_3$.⁶ Upon illumination by a laser light in the creep phase, the creeping current increases, and the external voltage required for the dynamic phase transition to the sliding phase becomes higher. In the sliding phase, the illumination can totally arrest the collective motion of the CDW under a modest external drive field. The effect vanishes when the excitation photon energy is below the single-particle gap⁷ of the $K_{0.3}MoO_3$. We attribute these photoeffects to a local and momentary destruction of the CDW order that leads to the phase slip and the redistribution of the CDW phase bypassing the pinning sites.

Sliding CDW materials are known to show unique memory effects⁸ because the phase configuration against the pinning sites can assume extremely complex form with nearly degenerate local minima.⁹ Once the CDW deforms

around a pinning site, it is hard to relax due to the potential from the nearby pinning sites, which results in the history-dependent response of the system. That is, the CDW response to the external field is governed by the internal deformation. This internal structure of the CDW was studied by several methods such as conductivity measurements on the multicontacted sample,¹⁰ electromodulated IR transmission,¹¹ and x-ray diffraction.¹²⁻¹⁵ The latter has a high resolution, and has been well exploited for many CDW materials.¹⁶ In this paper, we investigate the relation between the photoinduced dynamic phase transition and the CDW phase deformation in $K_{0.3}MoO_3$ directly by high-resolution x-ray scattering.

A CDW is accompanied by a lattice distortion of the form

$$\vec{u}(\vec{r}) = \vec{\Delta} \sin[\vec{Q} \cdot \vec{r} + \phi(\vec{r})], \quad (1)$$

where $\vec{Q} = 2\vec{k}_F$ is the CDW wave vector, $\vec{\Delta}$ is the amplitude of the complex CDW order parameter, and ϕ is the position-dependent phase. With some approximation, the intensity of the first CDW satellite peak at a scattering vector \vec{q} is proportional to the spatial Fourier transform of the exponential phase-phase correlation function,¹⁷

$$I(\delta\vec{q}) \sim |J_1(\vec{q} \cdot \vec{\Delta})|^2 \int d\vec{r} e^{i\delta\vec{q} \cdot \vec{r}} \langle e^{i[\phi(\vec{r}) - \phi(\vec{0})]} \rangle, \quad (2)$$

where $\delta\vec{q} = \vec{q} - (\vec{G} \pm \vec{Q})$, \vec{G} is a reciprocal-lattice vector and $J_1(x)$ is the Bessel function of order 1. The correlation function in Eq. (2) dominates the satellite peak profile. Basically one can imagine two types of the peak profile change: peak shift and broadening.¹² For our experimental geometry described below, we can attribute the peak shift to the tilt of the CDW phase front, while the broadening is inversely proportional to the CDW phase-coherence length normal to the chain [the $(2a^*c^*)$ direction]. Experimentally, a broadening of the CDW satellite peaks in $K_{0.3}MoO_3$ was observed in the presence of electric field around or larger than the threshold of the sliding conduction.^{12,13} In some cases, a shift or

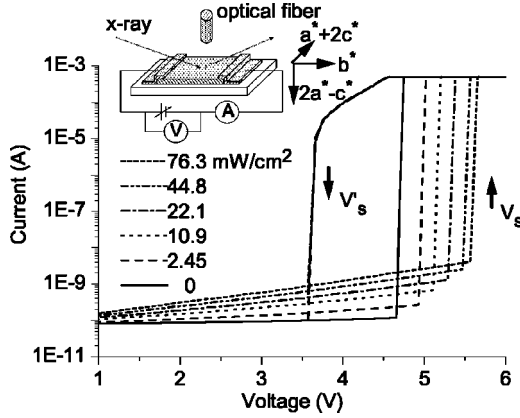


FIG. 1. Photoinduced change of the I - V characteristics measured at 12 K. The creep-to-slide transition voltage (V_s) and the creep current (below V_s) increase with the illumination intensity. The current is limited at $500 \mu\text{A}$ for the sample protection and to avoid Joule heating. The inset shows the electrical contact arrangement, the optical fiber for the light illumination, and the x-ray scattering geometry.

split of the satellite peak, accompanied by the broadening, along the $(2a^*-c^*)$ direction, was observed^{14,15} and usually attributed to the inhomogeneity of the electric field in the sample.¹⁸ $(2a^*-c^*)$ is perpendicular to both the one-dimensional structure and the cleavage plane of $\text{K}_{0.3}\text{MoO}_3$.

II. EXPERIMENT

$\text{K}_{0.3}\text{MoO}_3$ has a monoclinic structure with the space group $C2/m$, and the b -axis is parallel to the chains of MoO_6 octahedra.¹⁹ Sample crystals are synthesized by means of the electrolytic reduction of a KMoO_4 - MoO_3 melt.²⁰ The typical sample size is $1.3 \times 1 \times 0.2 \text{ mm}^3$. Indium electrodes were evaporated onto a freshly cleaved surface. The sample was glued to a sapphire plate and mounted in a closed-cycle refrigerator.

Synchrotron x-ray-diffraction measurements were performed at beam line-4C at the Photon Factory, KEK, Tsukuba. The incident beam is monochromated by a Si(111) double crystal, and focused on the sample position by a bent-cylindrical mirror. An x ray with an energy of 10 keV was used. The resolutions estimated from the Bragg reflection of $(12, 0, -6)$, which is nearby the measured superlattice peak, were 0.0037 and 0.0019 \AA^{-1} along the $(2a^*-c^*)$ and b^* directions, respectively. The sample was set so that the scattering plane is parallel to the $(2a^*-c^*)$ - b^* reciprocal plane.

III. RESULTS AND DISCUSSION

A. I - V characteristics

I - V characteristics of the sample measured at 12 K are shown in Fig. 1. As is often observed at low temperature,¹ a clear switching behavior at V_s with increasing applied voltage, and a hysteresis behavior at V'_s with decreasing voltage, can be seen (the current is limited to $500 \mu\text{A}$ to protect the sample). Below V_s , the current is carried by the creeping motion of the CDW.²¹ The observed switching corresponds

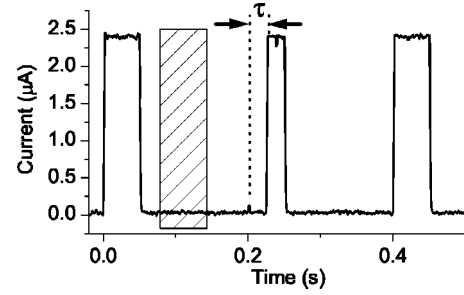


FIG. 2. Photoinduced switching delay measured at 12 K. Unipolar voltage pulses (6 V , 5 Hz , and 50 ms in duration) were applied to the sample, and the current was measured by the reference resistor of $1 \text{ M}\Omega$ inserted in the circuit. With laser irradiation (50 mW/cm^2 , 70 ms , indicated by shaded box), the onset of the sliding motion develops a delay τ for the following pulse.

to the creep-to-slide dynamic phase transition, as reported earlier.⁶ The voltage at the deformed solid to the plastic creep phase transition is about three orders of magnitude smaller than V_s (Ref. 13), therefore, we cannot resolve it. With a weak light illumination (photon energy 2.33 eV), the creep current increases and the sliding voltage V_s becomes higher. With increasing illumination intensity, V_s increases monotonically. Clearly, optical excitation affects the dynamic phase transition of the CDW from creep to slide. We attribute these optical effects to the photoinduced phase slip and the redistribution of the formerly deformed CDW phase, which stabilize the creeping phase.

The contact arrangement is shown in the inset of Fig. 1. As discussed by Tamegai *et al.*,¹⁵ the electric field in the sample can be inhomogeneous, leading to the largest strain of the CDW phase at the sample surface. This is convenient to study the relation between the CDW strain and the photoinduced dynamic phase transition, because the penetration depth of the visible light is small ($\sim 0.1 \mu\text{m}$).²²

B. Conduction delay

Figure 2 shows the persistence of the photoexcitation effect. We applied the rectangular voltage pulses (5 Hz and 50 ms in duration) to the sample, and the transient current was measured by inserting a reference resistor of $1 \text{ M}\Omega$ to the circuit. With the light illumination (2.33 eV , 50 mW/cm^2 , and 70 ms in duration) between the voltage pulses, the onset of the sliding motion begins to exhibit a delay time τ . The CDW conduction delay was closely investigated by Levy and Sherwin,²³ and τ was interpreted as the time needed for the internal strain buildup toward the threshold for phase slippage. Their interpretation is consistent with our idea that photoexcitation leads to the redistribution of the CDW phase. The persistence of the photoeffect is strong evidence of the photoinduced change of the internal deformation. The change of the CDW internal structure by light illumination can be seen directly in the experiments shown below.

C. Diffraction measurements

We cooled the sample down to 12 K without applying external voltage, and investigated the profiles of the CDW

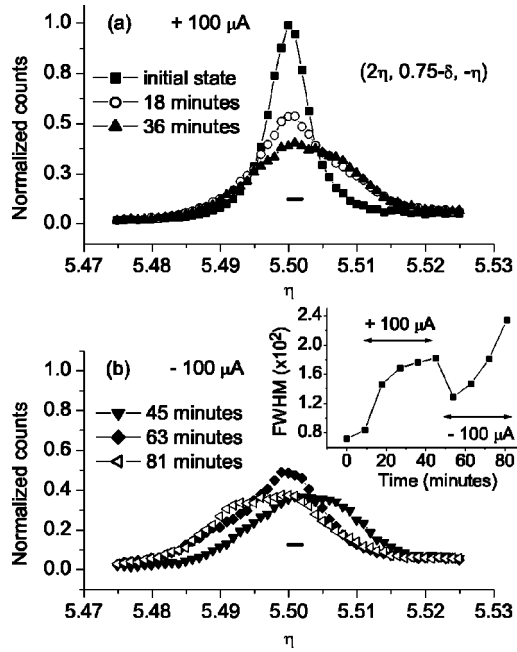


FIG. 3. Scans of the $(11, 0.75-\delta, -5)$ satellite peak in the $(2a^*-c^*)$ direction measured at 12 K. (a) Change of the peak profile by a constant current of $100 \mu\text{A}$. (b) After the 50 min of current application, the polarity of the current was reversed, and scans were taken successively. The inset shows the time evolution of the FWHM of the peak profiles. Solid lines are guides to the eye, and the horizontal bar indicates the resolution.

satellite peaks. Scans of the $(11, 0.75-\delta, -5.5)$ CDW satellite peak in the $(2a^*-c^*)$ direction are shown in Fig. 3. δ indicates the small deviation of \bar{Q} from the commensurate value of 0.75. Data are normalized by the peak height of the profile before the application of the electric field (we defined this as an initial state). With a constant current of $100 \mu\text{A}$ applied to the sample at a time 0, a clear shift of the peak position and a broadening of the profile were observed as reported earlier.^{12–15} The observed evolution of the internal deformation was slow, and the height of the peak profile reduced to the half-count of the initial value in about 20 min. 50 min after the application of the current, we reversed the polarity of the current [Fig. 3(b)]. Then the peak began to move to the opposite direction. The time evolution of the full width at half maximum (FWHM) of the peak profile is shown in the inset of Fig. 3(b). The FWHM of the peak profile slightly recovered due to the change in the current polarity, but never recovered to its initial value, and began to increase further with the duration of the current application. These results are consistent with those of previous reports. After the current was removed, a small relaxation of the peak profile was observed, as discussed below (we refer to this as thermal relaxation hereafter). The peak profile can be totally recovered only through the thermal cycling above the Peierls transition temperature ($T_p = 183 \text{ K}$).

To distinguish the photoinduced change of the internal deformation from the thermal relaxation, we measured the peak profile in the following sequence: (1) we cooled the sample without external field (initial state), (2) we applied an

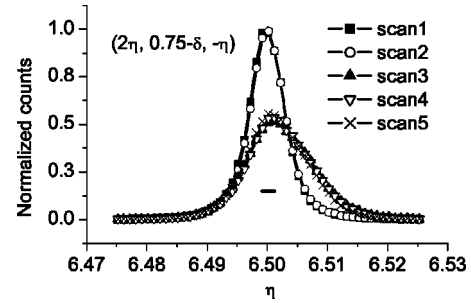


FIG. 4. Scans of the $(13, 0.75-\delta, -6)$ satellite peak in the $(2a^*-c^*)$ direction measured at 12 K. Two and three nearly overlapping curves are shown: a cooled state without an external field (scan 1), with a voltage of $1 \text{ V} (< V_s)$ in the creep phase (scan 2), after the application of $6 \text{ V} (> V_s)$ for 9 min (scan 3), 36 min after the removal of the voltage (scan 4), and immediately after the application of light (1.84 eV , 56 mW/cm^2) (scan 5). Solid lines are guide to the eye, and the horizontal bar indicates the resolution.

electric field of $1 \text{ V} (< V_s)$ to investigate the CDW deformation in the creep phase, (3) we applied an electric field of $6 \text{ V} (> V_s)$ for about 9 min to induce a large internal deformation in the sample, (4) we measured the thermal relaxation until it subsided (it took about 40 min), and (5) we illuminated the sample with a laser light (1.84 eV , 56 mW/cm^2). After each procedure, one peak profile was measured, each profile being called as scan 1, scan 2, etc.

Successive scans of $(13, 0.75-\delta, -6.5)$ CDW satellite peak in the $(2a^*-c^*)$ direction are shown in Fig. 4. Small change of the peak profiles after the procedures (2), (4), and (5) are barely discernible. To investigate the observed change closely, we took differential profiles between two successive scans, viz. 2-1, 4-3, and 5-4, as shown in Figs. 5(a)–5(c), respectively. In the creep phase [Fig. 5(a)], the shift of the peak profile toward a higher wave number can be seen, similar to that observed in the sliding phase. For the thermal relaxation [Fig. 5(b)], the recovery of the peak profile is of the same order of magnitude as that of the creep motion, but the shape of the difference profile is nearly symmetric with respect to $\eta = 0.65$, and looks like a second derivative of the peak. In Fig. 5(c), a photoinduced shift (a first-derivative-like shape) of the peak profile toward a lower wave number can be clearly observed. This photoinduced change occurs immediately after the application of the laser light.

After the application of the laser light, we executed the thermal cycling up to 50 K to investigate the thermal relaxation of the CDW internal deformation. The observed change of the peak profile is shown in Fig. 6. The narrowing of the FWHM indicates the recovery of phase coherence in the $(2a^*-c^*)$ direction. The difference profile is nearly symmetric with respect to $\eta = 6.50$, and similar to the shape shown in Fig. 5(b). Therefore, the relaxation of the internal deformation after the removal of external field seen in Fig. 5(b) should result from the phase relaxation caused by the thermal fluctuation.

D. Discussion

We first discuss the effect of the Joule heating and the laser heating. We have investigated the peak profiles of the

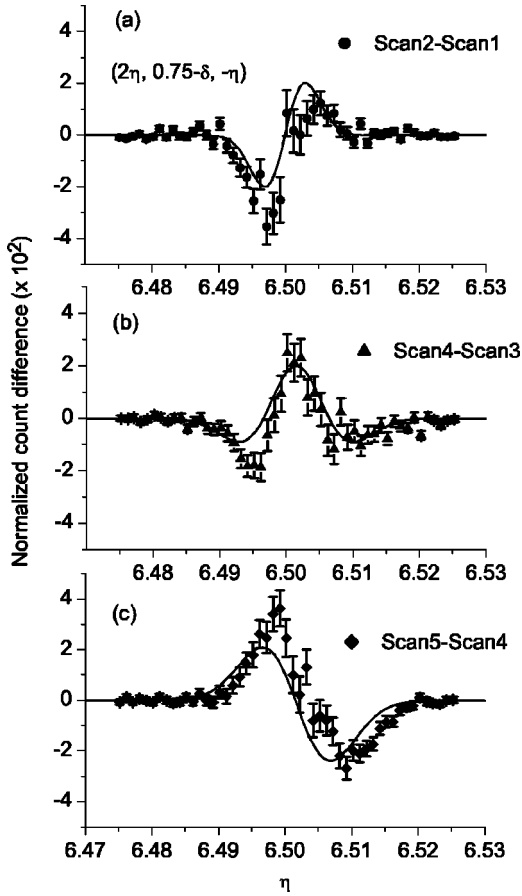


FIG. 5. The difference profiles of the superlattice peak shown in Fig. 4. (a) Difference between the profiles of scan 2 and scan 1, indicating the tilt of the phase front in the creep phase. (b) Difference between scan 4 and scan 3, indicating the thermal relaxation. (c) Difference between scan 5 and scan 4, which shows the photo-induced relaxation of the phase front. Each profile is fitted with the first or second derivative of the Gaussian function (solid lines).

(12, 0, -6) Bragg reflection with and without a simultaneously applied current of 500 μ A, and confirmed that the shift of the satellite peak through the lattice expansion from Joule heating can be negligible. With a light illumination of 100 mW/cm^2 , the temperature rise of the sample surface

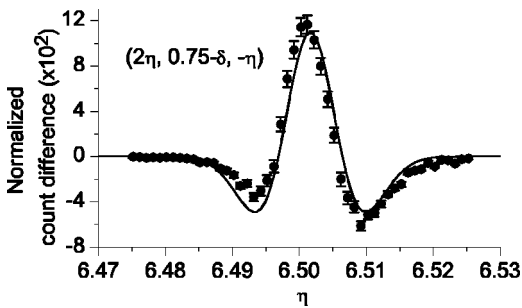


FIG. 6. The relaxation of the CDW internal deformation by the thermal cycling up to 50 K. The narrowing of the peak profile indicates the recovery of the phase coherence in the $(2a^*-c^*)$ direction. The solid line shows the fit by a second derivative of the Gaussian function.

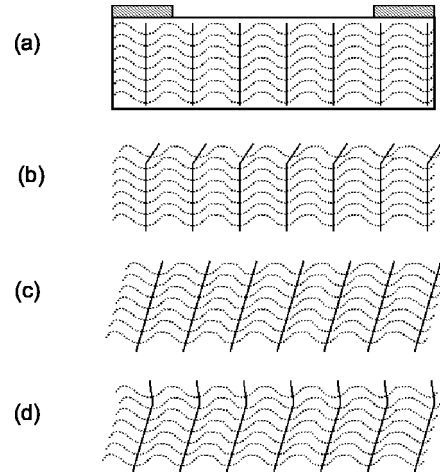


FIG. 7. A schematic picture of the tilting of the CDW phase front in the $(2a^*-c^*)$ direction. The effect of phase coherence (local or in-chain distortion) is not depicted. (a) Cooled state without external voltage. (b) In the creep phase; deformation occurs only near the sample surface. (c) After the application of the external voltage larger than V_s . (d) After the light illumination; the CDW phase near the sample surface is reconstructed.

can be estimated to be less than 0.01 K for our experimental condition using the known thermal conductivity.²⁴ So our present measurements are free from heating effects.

As mentioned earlier, the observed profiles of the CDW satellite peaks are dominated by two factors: a tilt of the CDW phase front and a loss of coherence of the CDW phase; each causes a peak shift and a broadening of the peak profile, respectively. The peak profiles in Fig. 4 can be fitted with Gaussian functions. Therefore, the shift and broadening of the peak profile shown in Fig. 5 can be expressed with the first and second derivatives of the Gaussian peak profile, respectively. In the creep phase, the difference profile [Fig. 5(a)] can be fitted with the first derivative of the initial (scan 1) Gaussian profile. Considering the electrode arrangement and the least electric conductivity in the $(2a^*-c^*)$ direction, the electric field is expected to be large along the sample surface [the $b^*-(a^*+2c^*)$ plane] but not so deep in the sample. Therefore, the asymmetric shape of the difference profile can be explained by the small tilt of the phase front near the sample surface, leaving the phase coherence in the $(2a^*-c^*)$ direction largely unaffected [Fig. 7(b), where the local distortions leading to the reduced coherence are not depicted]. With the external voltage larger than V_s , many parts of the CDW wave front tilt in proportion to the electric field in the sample [Fig. 7(c)]. When we remove the voltage, thermal relaxation occurs. The difference profile in Fig. 5(b) can be fitted with the second derivative of the Gaussian profile of scan 3, indicating the recovery of the phase coherence rather than the recovery of the tilt of the phase front. Considering the penetration depth of the visible light [$\sim 0.1 \mu\text{m}$ (Ref. 22)], which is about 100 times smaller than the penetration depth of the x-ray in our experimental setup ($\sim 12 \mu\text{m}$), the photoinduced change of the CDW deformation occurs only near the sample surface. The difference profile in Fig. 5(c) can be fitted by the first derivative of the

Gaussian profile of scan 4, indicating the recovery of the tilt of the phase front within the penetration depth of the visible light [Fig. 7(d)].

The magnitude of the difference profile [up to 4% of the total peak height; see Fig. 5(c)] indicates the existence of the relatively large deformation in the sample surface, which can be removed by light. The absolute amplitude of the difference profile in Figs. 5(a) and 5(c) are nearly the same, while the direction is just the opposite. This demonstrates that the light illumination can remove the considerable part of the strain incurred in the creep state. Because the accumulation of the strain in the creep phase is the decisive factor for the creep-to-slide dynamic phase transition, the pronounced effects of light illumination in Figs. 1 and 2 are quite reasonable. The peak profile immediately shifts due to light application, in contrast to the slow shift incurred by the external voltage or by the thermal relaxation, which is consistent with the idea of single-particle excitation.²⁵

Above data are all consistent with our interpretation of the photoexcited dynamic phase transition;⁶ incident photons happen to destroy the condensate in the highly distorted region around pinning sites near the sample surface, and the excited quasiparticles should recondense into a less deformed phase configuration, bypassing the pinning potential, leading to the relaxation of the phase strain and to the stabilization of the creep phase. The smallness of the penetration depth of the visible light shows that the condition of the

CDW phase in the most strained region (the sample surface in our case) dominates the dynamics of the creep to slide phase transition.

IV. CONCLUSION

In conclusion, we investigated the optical change of the CDW phase structure by high-resolution x-ray scattering. We found that the satellite peak of the CDW shifts in the creeping flow phase and shifts back with the photoexcitation. The dynamic phase transition in the CDW from a creeping state to a sliding state can be drastically affected by the condition of the CDW phase deformation within the penetration depth of the visible light.

ACKNOWLEDGMENTS

We thank Professor S. Kagoshima, Professor N. Nagao, Professor T. Tamegai, and Professor H. Matsukawa for valuable comments and discussions, Dr. H. Nakao, Dr. H. Ohsumi, and Dr. M. Kubota for their help in the experiments made at the synchrotron radiation facility in KEK, and R. Kondo for his help in sample preparation. The work was supported in part by Grant-in-Aid for COE Research of the Ministry of Education, Culture, Sports, Science and Technology, Japan.

*Electronic mail: stream@myn.rcast.u-tokyo.ac.jp

¹For a review, see, for example, G. Grüner, *Rev. Mod. Phys.* **60**, 1129 (1988); G. Grüner, *Density Waves in Solids*, (Addison-Wesley, Reading, MA, 1994).

²G. Blatter, M.V. Feigel'man, V.B. Geshkenbein, A.L. Larkin, and V.M. Vinokur, *Rev. Mod. Phys.* **66**, 1125 (1994).

³L. Balents and M.P.A. Fisher, *Phys. Rev. Lett.* **75**, 4270 (1995).

⁴See, for example, Stefan Scheidl, and Valerii M. Vinokur, *Phys. Rev. E* **57**, 2574 (1998).

⁵F. Pardo, F. de la Cruz, P.L. Gammel, E. Bucher, and D.J. Bishop, *Nature (London)* **396**, 348 (1998).

⁶N. Ogawa, A. Shiraga, R. Kondo, S. Kagoshima, and K. Miyano, *Phys. Rev. Lett.* **87**, 256401 (2001).

⁷G. Travaglini, P. Wachter, J. Marcus, and C. Schlenker, *Solid State Commun.* **37**, 599 (1981).

⁸R.M. Fleming and L.F. Schneemeyer, *Phys. Rev. B* **28**, 6996 (1983); **33**, 2930 (1986).

⁹P.B. Littlewood, *Phys. Rev. B* **33**, 6694 (1986); P.B. Littlewood and R. Rammal, *ibid.* **38**, 2675 (1988).

¹⁰S.G. Lemay, M.C. de Lind van Wijngaarden, T.L. Adelman, and R.E. Thorne, *Phys. Rev. B* **57**, 12 781 (1998); S.G. Lemay, K. O'Neill, C. Cicak, and R.E. Thorne, *ibid.* **63**, 081102 (2001).

¹¹M.E. Itkis, B.M. Emerling, and J.W. Brill, *Phys. Rev. B* **52**, R11545 (1995).

¹²R.M. Fleming, R.G. Dunn, and L.F. Schneemeyer, *Phys. Rev. B* **31**, 4099 (1985).

¹³Laszlo Mihaly, Ki-Bong Lee, and Peter W. Stephens, *Phys. Rev.*

B **36**, 1793 (1987).

¹⁴J. Zhang, J.F. Ma, S.E. Nagler, and S.E. Brown, *Phys. Rev. B* **47**, 1655 (1993).

¹⁵T. Tamegai, K. Tsutsumi, S. Kagoshima, M. Sato, K. Tsuji, J. Harada, M. Sakata, and T. Nakajima, *Solid State Commun.* **51**, 585 (1984).

¹⁶See, for example, H. Requardt, F.Ya. Nad, P. Monceau, R. Currat, J.E. Lorenzo, S. Brazovskii, N. Kirova, G. Grübel, and Ch. Vettier, *Phys. Rev. Lett.* **80**, 5631 (1998); S. Brazovskii, N. Kirova, H. Requardt, F.Y. Nad, P. Monceau, R. Currat, J.E. Lorenzo, G. Grubel, and C. Vettier, *Phys. Rev. B* **61**, 10640 (2000).

¹⁷D. DiCarlo, R.E. Thorne, E. Sweetland, M. Sutton, and J.D. Brock, *Phys. Rev. B* **50**, 8288 (1994); A.W. Overhauser, *ibid.* **3**, 3173 (1971).

¹⁸T. Tamegai, K. Tsutsumi, and S. Kagoshima, *Physica B & C* **143**, 114 (1986).

¹⁹J. Graham and A.D. Wadsley, *Acta Crystallogr.* **20**, 93 (1966).

²⁰A. Wold, W. Kunmann, R.J. Arnott, and A. Ferretti, *Inorg. Chem.* **3**, 545 (1964).

²¹S.G. Lemay, R.E. Thorne, Y. Li, and J.D. Brock, *Phys. Rev. Lett.* **83**, 2793 (1999).

²²L. Degiorgi, B. Alavi, G. Mihaly, and G. Grüner, *Phys. Rev. B* **44**, 7808 (1991).

²³J. Levy and M.S. Sherwin, *Phys. Rev. B* **43**, 8391 (1991).

²⁴R.S. Kwok and S.E. Brown, *Phys. Rev. Lett.* **63**, 895 (1989).

²⁵J. Demsar, K. Biljalovic, and D. Mihailovic, *Phys. Rev. Lett.* **83**, 800 (1999).